ACS Catalysis

Research Article

pubs.acs.org/acscatalysis

Kinetics and Mechanism of Ethanol Dehydration on γ-Al_2O_3: The Critical Role of Dimer Inhibition

Joseph F. DeWilde,[†,§] Hsu Chiang,[†,§] Daniel A. Hickman,[‡] Christopher R. Ho,[†] and Aditya Bhan*[,†]

[†]Department of Chemical Engineering and Materials Science, University of Minnesota-Twin Cities, 421 Washington Avenue SE, Minneapolis, Minnesota 55455, United States

[‡]Engineering and Process Science, The Dow Chemical Company, 1776 Building, Office A-17, Midland, Michigan 48674, United States

Supporting Information

ABSTRACT: Steady state, isotopic, and chemical transient studies of ethanol dehydration on γ-alumina show unimolecular and bimolecular dehydration reactions of ethanol are reversibly inhibited by the formation of ethanol−water dimers at 488 K. Measured rates of ethylene synthesis are independent of ethanol pressure (1.9−7.0 kPa) but decrease with increasing water pressure (0.4−2.2 kPa), reflecting the competitive adsorption of ethanol−water dimers with ethanol monomers; while diethyl ether formation rates have a positive, less than first order dependence on ethanol pressure (0.9−4.7 kPa) and also decrease with water pressure (0.6−2.2 kPa), signifying a competition for active sites between ethanol−water dimers and ethanol dimers. Pyridine inhibits the rate of ethylene and diethyl ether formation to different extents verifying the existence of acidic and nonequivalent active sites for the dehydration reactions. A primary kinetic isotope effect does not occur for diethyl ether synthesis from deuterated ethanol and only occurs for ethylene synthesis when the β-proton is deuterated; demonstrating olefin synthesis is kinetically limited by either the cleavage of a C_β-H bond or the desorption of water on the γ-alumina surface and ether synthesis is limited by the cleavage of either the C−O bond of the alcohol molecule or the Al−O bond of a surface bound ethoxide species. These observations are consistent with a mechanism inhibited by the formation of dimer species. The proposed model rigorously describes the observed kinetics at this temperature and highlights the fundamental differences between the Lewis acidic γ-alumina and Brønsted acidic zeolite catalysts.

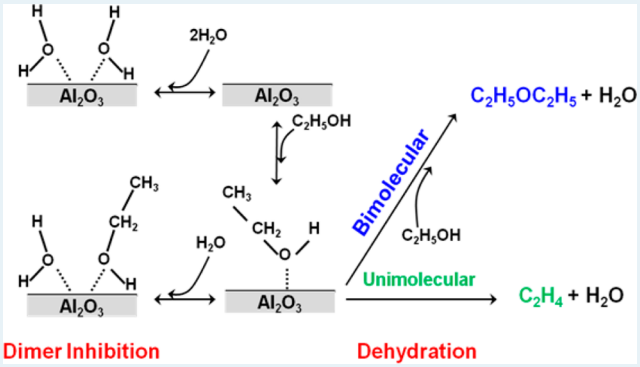

KEYWORDS: *ethanol dehydration, γ-alumina, parallel reactions, surface dimer species, ethylene, diethyl ether, Lewis acid sites*

1. INTRODUCTION

Gamma alumina (γ-Al_2O_3) is an industrially relevant solid catalyst because of its high surface area (50−300 m^2 g^{-1}) and thermal stability up to 873 K.[1−5] Alcohols dehydrate over γ-Al_2O_3 to form either olefins or ethers through unimolecular or bimolecular pathways, respectively; both pathways result in the production of water as a byproduct.[6,7] The dehydration of alcohols over γ-Al_2O_3, thus, can serve as a probe to elucidate the catalytic site requirements and molecular reaction mechanisms on this important material.

The surface of γ-Al_2O_3 contains hydroxyl groups, Lewis acid sites in the form of surface aluminum (Al) atoms, as well as surface oxygen (O) atoms capable of behaving as basic sites.[8−10] Pyridine is often used a basic probe molecule to titrate both Brønsted and Lewis acid sites on catalytic surfaces.[11−13] The infrared spectroscopic band associated with the presence of pyridinium ions on the surface of pyridine-exposed γ-Al_2O_3 samples (1540 cm^{-1}) was not observed by Parry[11] at ambient temperatures while a band associated with pyridine bonded to Lewis acid sites (1450 cm^{-1}) was observed, leading the authors to conclude that surface hydroxyl groups are unable to protonate pyridine and, by extension, the less basic alcohol molecules, thereby demonstrating that acid sites required for alcohol dehydration over γ-Al_2O_3 are likely to be Lewis acidic rather than Brønsted acidic. Upon evacuation of the sample at 423 K, Parry[11] observed the band at 1450 cm^{-1} split into two distinct bands verifying the existence of multiple Lewis acid sites on γ-Al_2O_3. The conclusion that γ-Al_2O_3 is not Brønsted acidic is further supported by ^{15}N Nuclear Magnetic Resonance (NMR) measurements on pyridine exposed γ-Al_2O_3 performed by Ripmeester[14] in which the pyridinium ion (peak at 170 ppm) was also not observed. Additionally, Kwak et al.[15] observed a near 1:1 correlation with the decrease in the intensity of the ^{27}Al NMR peak attributed to surface penta-coordinated aluminum atoms (~23 ppm) and the BaO loading of BaO loaded γ-Al_2O_3 samples, indicating that BaO acts as a

Received: January 23, 2013
Revised: March 11, 2013
Published: March 26, 2013

selective titrant of penta-coordinated alumina atoms. Furthermore, Kwak et al.[16] observed the dehydration rates of methanol into dimethyl ether on BaO/γ-Al_2O_3 at 573 K decreased with BaO loading, suggesting that Lewis acidic penta-coordinated surface alumina atoms play an important role in the synthesis of ethers from alcohol dehydration on γ-Al_2O_3.

Pines and Haag[17] found that the cis/trans ratio among 2-butene isomers produced from 2-butanol dehydration (cis/trans = 4.3) was nearly equivalent to that from 1-butene double-bond isomerization (cis/trans = 4.4) over η-alumina at 523 K; on this basis the authors concluded that the two reactions occur through the same intermediate. The authors proposed a proton olefin complex on the surface formed from the decomposition of a surface bound oxonium ion as the intermediate for olefin formation to explain the high cis/trans ratios observed. Knözinger and Scheglila[18] alternatively concluded olefin formation occurs through an E-2 type elimination of the alcohol rather than through a proton-olefin complex intermediate based upon the measured kinetic isotope effects (KIE) for the dehydration of deuterated *tert*-butanol, *sec*-butanol, and *iso*-butanol into butenes between 393 and 483 K. Knözinger et al.[19] proposed the alcohol undergoes this elimination across a surface hydroxyl group and a basic center. An olefin in absence of water, however, would be unable to reform the proposed reaction intermediate; the active sites, therefore, would not be appropriate for olefin double bond isomerization. Thus the mechanism proposed by Knözinger et al.[19] is unable to fully explain the same cis/trans ratios for dehydration and double bond isomerization measured by Pines and Haag.[17]

Steady state kinetic measurements performed by Knözinger et al. on the rate of olefin formation from the dehydration of cyclohexanol[20] (10−33 kPa at 433 and 453 K) and the rate of ether formation from the dehydration of methanol[21] (7−35 kPa methanol pressures at 433−468 K) over γ-Al_2O_3 with varying alcohol and water partial pressures showed that the rates of olefin and ether synthesis were inhibited by water and increased with alcohol pressure before becoming independent of alcohol pressure. The empirical rate expression shown in eq 1 was proposed by the authors to fit the resulting data for both reactions.

$$r = r_0 \frac{\sqrt{P_A}}{\sqrt{P_A} + bP_W} \quad (1)$$

r is the rate of olefin or ether formation, r_0 is the rate of olefin or ether formation at the zero order in the alcohol pressure limit, P_A and P_W are the partial pressures of alcohol and water, respectively, and b is an empirical constant. The square root dependence on ethanol pressure of the proposed expression, however, implies the dissociation of the alcohol molecule into two equivalent surface species, which is not consistent with their proposed mechanisms for dehydration. Conversely, Shi and Davis[22] observed, upon dehydration of 2-butanol and methanol at a constant total alcohol pressure at 503 K, the selectivity of di-2-butyl and dimethyl ether increased proportionally with the square of the partial pressure of 2-butanol and methanol, respectively. Alternatively, De Morgues et al.[23] proposed that olefin formation occurred over two sites, one of which is inhibited by water surface species based upon their observation that the rate of propene synthesis from 2-propanol dehydration was inversely proportional to water pressure (in the range of 0.0 to 1.2 kPa) and independent of 2-propanol pressure (in the range of 1.1 to 3.1 kPa) between 373 and 433 K. A mechanism consistent with the observed inhibitory kinetic effects of water and the pressure dependence of both ether and olefin synthesis rates on alcohol pressure has not been reported in the literature.

In this work, steady state kinetic measurements demonstrate ethylene and diethyl ether (DEE) synthesis from the dehydration of ethanol over γ-Al_2O_3 at 488 K are both inhibited by the formation of ethanol−water dimer species at ethanol pressures between 1.9 and 7.0 kPa and water partial pressures between 0.4 and 2.2 kPa. Water was determined to irreversibly poison a fraction of the active sites for ethylene and DEE formation. Pyridine was found to reversibly inhibit the rate of both ethylene and DEE synthesis to different degrees, indicating the active sites are acidic in nature and are not identical for the two dehydration products. Kinetic mechanisms consistent with these conclusions are presented and evaluated.

2. MATERIALS AND METHODS

2.1. Catalyst Preparation. γ-Al_2O_3 (Alfa Aesar, BET surface area = 155 m^2/g^{-1}, pore volume = 0.257 $cm^3\ g^{-1}$) was treated for 3 h in a 1 M NH_4NO_3 solution at 353 K prior to its use in kinetic experiments as previously described by Roy et al.[24] Catalyst particle sizes between 180 and 425 μm (40−80 mesh) were obtained by pressing and sieving the γ-Al_2O_3 powder. Acid-washed quartz sand (0.5−0.7 g, 152−422 μm particle size, Acros Organics) was mixed with the catalyst samples (0.02−0.2 g) to form the reactor bed. The catalyst was then treated in dry air (1.67 $cm^3\ s^{-1}$ at NTP conditions, Ind. Grade, Matheson Trigas) for 4 h at 723 K after heating the catalyst from ambient conditions with a rate of 0.0167 K s^{-1}. The catalyst samples were then cooled in dry air (1.67 $cm^3\ s^{-1}$) to the reaction temperature (488 K). The regeneration of the catalyst after kinetic experiments was also achieved using the same treatment in air.

2.2. Steady State Kinetic Measurements of Ethanol Dehydration over γ-Al_2O_3. The rate of ethanol dehydration was measured using a quartz tube packed bed reactor (10 mm inner diameter, 1.6 cm^3 bed volume) system. The bed temperature was measured with a type K thermocouple located on the external surface of the reactor and maintained at reaction temperature (488 K) using a tube furnace (National Electric Furnace FA120 type) and a Watlow temperature controller (96 series).

Ethanol dehydration was carried out at 488 K and ambient pressure under a carrier gas consisting of He (1.7−3.2 $cm^3\ s^{-1}$ at NTP conditions, grade 4.7, Minneapolis Oxygen Company) and an internal standard mixture for analysis (25.0% CH_4 and balance Ar, 0.017 $cm^3\ s^{-1}$ at NTP conditions, Minneapolis oxygen) and under differential reaction conditions (<10% conversion). The catalyst was exposed to 2.2 kPa of deionized water diluted with the carrier gas (1.7 $cm^3\ s^{-1}$) for 1 h at 488 K prior to reaction.

Liquid pyridine (99+%, Sigma Aldrich), C_2H_5OH (99.5%, Decon Laboratories, Inc.), C_2H_5OD (99.5 at.% D, Sigma-Aldrich), C_2D_5OD (99.5 at.% D, Sigma-Aldrich), and deionized water were fed into the carrier gas stream at 405 K via syringe pumps (KD scientific KDS −100 and Cole Parmer). Feed partial pressures (0.0−0.3 kPa pyridine, 0.9−7.0 kPa C_2H_5OH, 1.3 kPa C_2H_5OD, 1.0 kPa C_2D_5OD, and 0.4−2.3 kPa deionized water) were controlled by adjusting the liquid flow rates into the system. Condensation of the reactants and products was

dx.doi.org/10.1021/cs400051k | ACS Catal. 2013, 3, 798−807

avoided via the resistive heating of the transfer lines to temperatures greater than 343 K.

The composition of the reactor effluent was analyzed using an online mass spectrometer (MKS Cirrus 200 Quadrupole) and a gas chromatograph (Agilent 6890 N GC) with both a flame ionization detector fed through a methyl-siloxane capillary column (HP-1, 50.0 m × 320 μm × 0.52 μm) and a thermal conductivity detector fed through a packed column (SUPELCO HAYESEP R 80/100 mesh packed column, 12 ft). Error bars in the reported figures correspond to the 95% confidence intervals based upon successive gas chromatograph injections taken without changing the experimental conditions.

A reactor containing only quartz sand diluent (0.793 g) generates, on average, 1.1×10^{-9} mol s^{-1} of DEE and no ethylene upon feeding ethanol (2.6 kPa) and water (1.1 kPa) at 488 K. The production of DEE on the quartz sand diluent (~10% of the total rate of DEE production) was accounted for and removed when calculating the reported rates of DEE synthesis. Exposure to pyridine (0.1 kPa) was observed to completely and irreversibly deactivate the production of DEE on the diluent alone; the rate of DEE production was, therefore, not adjusted in measurements in which pyridine was cofed with ethanol (Section 3.2).

2.3. In-Situ Chemical Titration of Diethyl Ether Active Sites Using Pyridine. Pyridine (0.02 and 0.05 kPa) was introduced to a reactant stream containing ethanol (1.5 kPa) and water (1.1 kPa) flowing over 0.2 g of catalyst (exposed to 2.2 kPa of water at 488 K for 1 h) at 488 K, and the resulting transient production of DEE was monitored using an in-line mass spectrometer (MKS Cirrus 200 Quadrupole mass spectrometer system). The pyridine uptake that would eliminate DEE synthesis was determined by extrapolating the deactivation profile (see section 3.2).

2.4. Parameter Estimation Techniques for Kinetic Modeling. Kinetic parameters were optimized and uncertainties (95% marginal highest posterior density intervals) were determined using the Athena Visual Studio (v14.2, W. E. Stewart and M. Caracotsios) statistical software package and Bayesian statistical estimation techniques. Replicates for fit analysis were provided by independent kinetic measurements at the same ethanol and water pressure but for experimental measurements taken at constant water or constant ethanol pressure discussed in Section 3.4.

3. RESULTS AND DISCUSSION

3.1. Effects of Prior Exposure of γ-Al_2O_3 to Water on Ethanol Dehydration Rates. The rates of ethylene and diethyl ether synthesis from the dehydration of ethanol at 488 K were found to be 59 and 34% lower, respectively, for catalyst samples that have undergone treatment in water prior to reaction (exposed to 2.2 kPa of water at 488 K for 1 h) than catalyst samples which have not (Table 1), demonstrating water is capable of deactivating some of the active sites and inhibiting the rate of ethylene and DEE formation either by irreversibly adsorbing onto the active sites or by causing a structural change in the surface of the catalyst. This conclusion is supported by the Temperature Programmed Desorption (TPD) experiments performed by Roy et al.[24] in which the amount of 2-propanol adsorbed onto the surface of their γ-Al_2O_3 samples was found to be 73% lower for samples with prior exposure to water (exposed to 0.4 kPa water vapor at 373 K) than for samples without any prior water exposure. Additionally, Roy et al.[24] observed the temperature at which olefin was formed was

Table 1. Ethylene and DEE Synthesis Rates for Ethanol Dehydration at an Ethanol Pressure of 1.2 kPa and a Total Gas Flow Rate of 3.2 cm^3 s^{-1} over 0.02 g of γ-Al_2O_3 at 488 K for a Catalyst Sample Which Was Not Exposed to Water Prior to Reaction, A Catalyst Sample Exposed to 2.2 kPa Water for 1 h Prior to Reaction, and the Water Exposed Sample Regenerated in Air (1.67 cm^3 s^{-1} for 4 h at 723 K)

catalyst sample	ethylene synthesis rate ($/10^{-7}$ mol s^{-1} g^{-1})	DEE synthesis rate ($/10^{-6}$ mol s^{-1} g^{-1})
No H_2O exposure	2.22	5.29
H_2O exposed	0.90	3.49
regenerated	2.42	5.49

unchanged between the samples, leading the authors to conclude water simply blocked adsorption sites on the γ-Al_2O_3 surface rather than altering the structure of the active sites. Density Functional Theory (DFT) calculations (Perdew–Wang 91 generalized gradient-corrected exchange-correlation functional) by Digne et al.[25,26] and by Wischert et al.[27] both demonstrate water is capable of irreversibly disassociating on the under-coordinated aluminum atoms on the catalyst surface to form stable surface hydroxyl species, preferentially on highly under-coordinated (three- or four-coordinated) aluminum atoms.[25,26] Furthermore, Wischert et al.[27] observed that the number of sites for methane and hydrogen adsorption on γ-Al_2O_3 decreased with hydroxyl group coverage for samples pretreated at temperatures less than 923 K, demonstrating that these hydroxyl groups are capable of blocking potential catalytic active sites.

The rates of ethylene and DEE synthesis are restored upon treatment of the water exposed catalyst in air (1.67 cm^3 s^{-1}) for 4 h at 723 K (Table 1), demonstrating that thermal treatment can recover active sites for ethanol dehydration.

All subsequent experiments and measurements were performed on catalyst samples that have undergone water treatment to investigate the kinetics of ethanol dehydration in the absence of the irreversible deactivation caused by the water product.

3.2. Titration of Active Sites for Ethanol Dehydration. The rates of ethylene and DEE synthesis were observed to be inhibited by pyridine, but were found to return to the values measured prior to the introduction of pyridine after the pyridine feed was stopped (Figure 1a). These observations demonstrate the following: (1) either Lewis acidic Al atoms or hydroxyl groups comprise the active sites for both ethylene and DEE formation and (2) pyridine can reversibly bind to these active sites during ethanol dehydration, thus, inhibiting the reaction, but is incapable of irreversibly adsorbing onto these sites under reaction conditions.

The rate of formation of both ethylene and DEE normalized to the formation rate measured in the absence of a pyridine cofeed at different pyridine pressures is shown in Figure 1b. The rate of ethylene formation was found to be inhibited to a greater extent than the rate of DEE formation; indicating a difference in the equilibrium surface coverage of pyridine on the active sites of DEE and ethylene synthesis. The acidic active sites for ethylene and DEE synthesis are, therefore, not equivalent, although their uniqueness cannot be proven with inhibition experiments alone.

The amount of pyridine it would take to completely deactivate DEE synthesis was estimated by linearly extrapolating the initial slope of the measured DEE synthesis rate,

dx.doi.org/10.1021/cs400051k | ACS Catal. 2013, 3, 798–807

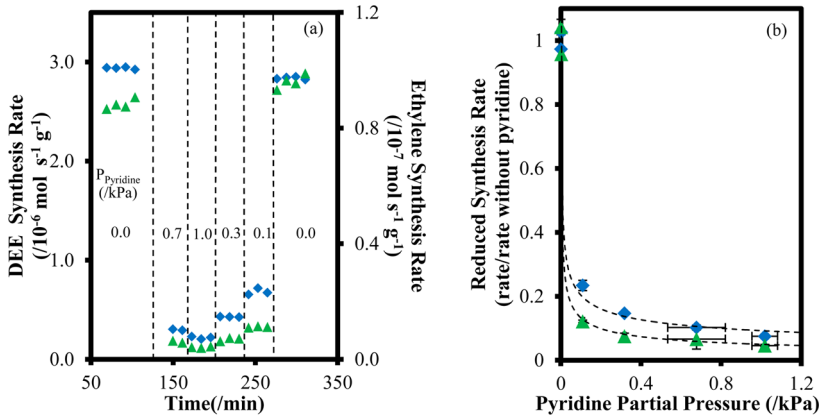

Figure 1. Ethylene (green triangles) and DEE (blue diamonds) (a) synthesis rates with respect to reaction time and (b) reduced synthesis rates normalized to the measured synthesis rates with no pyridine co-feed as a function of pyridine pressure for the dehydration of 0.9 kPa of ethanol over 0.02 g of γ-Al_2O_3 (total volumetric flow rate = 3.2 cm^3 s^{-1}) at 488 K. The dashed lines serve as a guide for the eye.

considering pyridine adsorption to be irreversible and all DEE active sites to exhibit similar activity in the linear regime (Figure 2). The residual synthesis of DEE is most likely a result

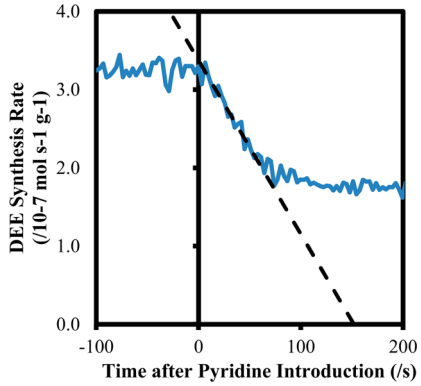

Figure 2. DEE synthesis rates as a function of time after introduction of 0.03 kPa of pyridine for the dehydration of ethanol (1.5 and 1.1 kPa ethanol and water partial pressures, respectively) over 0.2 g of γ-Al_2O_3 (total volumetric flow rate = 1.7 cm^3 s^{-1}) at 488 K. The dashed line shows the linear extrapolation used to determine pyridine uptake for complete deactivation.

of the dynamic reversibility of pyridine adsorption and inhibition demonstrated in Figure 1. On average, 2.7 × 10^{-5} mol g^{-1} (~0.10 sites nm^{-2}) of pyridine is estimated to completely deactivate DEE synthesis; this value is consistent across different pyridine pressures (0.02 and 0.05 kPa) and space velocities (1.1 and 2.0 s^{-1}) (Table 2). The number of pyridine adsorption sites for complete deactivation may not correlate directly with the number of active sites for DEE formation for two reasons: (1) it is possible that pyridine could adsorb onto sites other than the active sites for ethanol dehydration; and (2) the quantity of sites for either ethylene or DEE formation cannot be independently inhibited using an unspecific titrant such as pyridine.

Electron Paramagnetic Resonance measurements performed by Zotov et al.[28] on anthracene-exposed γ-Al_2O_3 samples determined ~0.002 molecules nm^{-2} of anthracene underwent radicalization on weak electron acceptor sites, which have been demonstrated to possess a linear correlation with the rate of ethylene formation from ethanol dehydration on doped γ-Al_2O_3 samples. The site density estimated by Zotov et al.[28] (~0.002 sites nm^{-2}) provides a lower bound to the active site density, as additional active sites for dehydration may exist that are not active for anthracene radicalization, while the estimation based upon in situ pyridine titration (~0.1 sites nm^{-2}) provides an upper bound to the active site density.

3.3. Kinetic Isotope Effects for Ethanol Dehydration.

The rates of ethylene and DEE formation from C_2H_5OH relative to the rates of formation using C_2D_5OD and C_2H_5OD (r_H/r_D) reactants at 488 K are presented in Table 3. No statistically significant effect on the rate of DEE formation is observed when using either deuterated reactant, demonstrating the rate-limiting step of DEE formation does not involve the cleavage of a C−H bond or the cleavage of one of the O−H bonds. Bimolecular dehydration of ethanol to form DEE, therefore, involves either the cleavage of the C_α-O bond or an Al−O bond in the rate-limiting step. Similarly, no kinetic isotope effects were observed by Knözinger et al.[29] for dimethyl

Table 2. Pyridine Uptake Necessary for Complete Deactivation of DEE Synthesis Rate Determined from in-situ Titrations Performed at Differing Pyridine Pressures and Space Velocities over 0.2 g of γ-Al_2O_3 at 488 K[a]

space velocity (/s^{-1})	pyridine pressure (/kPa)	pyridine uptake (/10^{-5} mol g^{-1})
1.1	0.05	2.7 ± 0.5
1.1	0.02	2.2 ± 0.9
2.0	0.05	3.2 ± 1.6
2.0	0.02	2.7 ± 0.3

[a]The 95% confidence intervals were determined based upon independent titrations.

Table 3. Measured Kinetic Isotope Effects for Ethylene and Diethyl Ether Formation at 488 K for the Dehydration of C_2H_5OD and C_2D_5OD over γ-Al_2O_3

	reactant	
product	C_2H_5OD[a]	C_2D_5OD[b]
ethylene KIE (r_H/r_D)	0.89 ± 0.14	2.42 ± 0.19
diethyl ether KIE (r_H/r_D)	0.97 ± 0.12	1.01 ± 0.14

[a]Reactions performed under 1.3 kPa of C_2H_5OH or C_2H_5OD with no water co-feed. [b]Reactions performed under 1.0 kPa of C_2H_5OH or C_2D_5OD with 1.2 kPa water co-feed.

dx.doi.org/10.1021/cs400051k | ACS Catal. 2013, 3, 798−807

ether formation from the dehydration of methanol, CH_3OD, and CD_3OD over γ-Al_2O_3.

No statistically significant difference was observed between the rates of ethylene formation from the dehydration of C_2H_5OH and C_2H_5OD, demonstrating O−H bond cleavage is not kinetically limiting for ethylene formation. A primary isotope effect, however, was observed for the dehydration of C_2D_5OD, verifying the rate-limiting step of ethylene formation involves either the breaking of a C−H bond (likely the more acidic C_β-H bond) or the desorption of a water molecule from the surface of the alumina in which a surface O−H bond is broken with the hydrogen atom originating from the ethanol molecule. Knözinger and Scheglila[18] similarly observed a primary kinetic isotope effect for *tert*-butanol, *sec*-butanol, and *iso*-butanol dehydration over γ-Al_2O_3 only when the C_β atom was deuterated.

3.4. Kinetics and Mechanism of Ethanol Dehydration. The formation rates of both ethylene and DEE formation were observed to be inhibited by water at 488 K; the rates of both DEE and ethylene synthesis, however, recovered to their initial value upon restoring the initial water pressure as shown in Figure 3, demonstrating water is capable of reversibly inhibiting ethylene and DEE synthesis in addition to irreversibly deactivating a fraction of the active sites of γ-Al_2O_3.

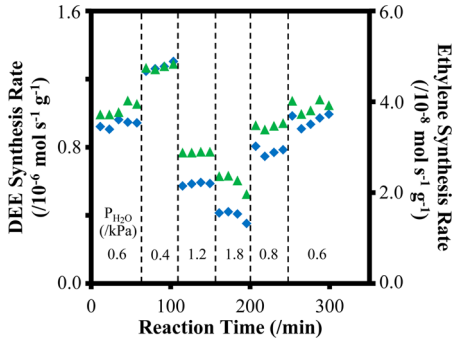

Figure 3. Ethylene (green triangles) and DEE (blue diamonds) synthesis rates from the dehydration of 4.2 kPa of ethanol over 0.02 g of γ-Al_2O_3 (total volumetric flow rate = 3.2 cm^3 s^{-1}) at 488 K as a function of reaction time and water pressure.

The rate of ethylene synthesis upon co-feeding ethanol and water at 488 K was found to be zero order with respect to ethanol pressure for the majority of the ethanol and water pressures investigated (between 1.9 and 7.0 kPa ethanol partial pressure and 0.4 and 2.2 kPa water partial pressure); becoming of positive order (0.4) in ethanol only at low ethanol pressures ($\leq$2 kPa) and at the tested highest water pressure (2.2 kPa) as shown in Figure 4a. A negative order dependence on water pressure for the rate of ethylene formation is still observed, however, in the regime where ethylene synthesis is invariant with ethanol pressure. These observations are consistent with the conclusion that the formation of ethylene must be inhibited at least partially by the formation of ethanol−water dimers to maintain the observed dependencies.

The inhibition of the rate of ethylene synthesis by water (0.4 to 1.9 kPa) was found to decrease with increasing ethanol pressure (0.9 to 4.2 kPa) and was found to have, on average, an order less than 1 (between −0.9 and −0.5) (Figure 5a). A competitive occupation of the surface sites by single molecule ethanol species, ethanol−water dimers, and water dimer surface species provides a consistent kinetic scheme capable of describing these observations.

A positive order dependence (between 0.0 and 0.8) in ethanol partial pressure was observed for the rate of DEE formation over the tested range of ethanol and water partial pressures (Figure 4b), with the exception of the highest tested ethanol pressures (>4 kPa) and the lowest tested water partial pressure (0.4 kPa), where the rate of DEE formation was found to be independent of ethanol pressure. The observed reaction order for DEE synthesis with respect to ethanol decreased with increasing ethanol pressure and decreasing water pressure. These observations can be explained by the competition between ethanol−water dimers and adsorbed ethanol dimers. This conclusion is further supported by the observation that the reaction order with respect to water pressure decreases with increasing ethanol pressure (0.9 to 4.2 kPa) from −1.3 to −0.7 (Figure 5b).

The rate of ethylene and DEE synthesis was found to be in the zero order regime with respect to ethanol pressure above 4 kPa of ethanol and at 0.4 kPa of water (Figure 4) despite ethylene synthesis being a unimolecular reaction and DEE synthesis being a bimolecular reaction; implying the active sites for ethylene and DEE formation are inhibited by different

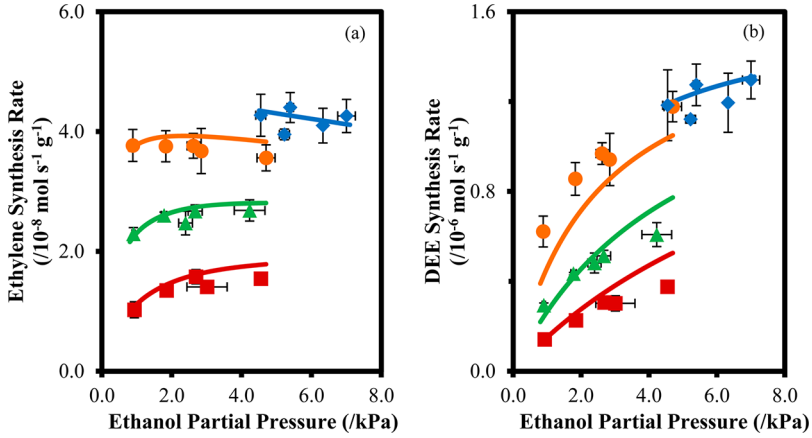

Figure 4. (a) Ethylene and (b) DEE synthesis rates for ethanol dehydration at 488 K on γ-Al_2O_3 as a function of ethanol partial pressure with 0.4 kPa (blue diamonds), 0.6 kPa (orange circles), 1.2 kPa (green triangles), and 2.2 kPa (red squares) water co-feeds (total gas flow rate = 3.2 cm^3 s^{-1}). The solid lines represent the model fits to equations (a) 3 and (b) 5.

dx.doi.org/10.1021/cs400051k | ACS Catal. 2013, 3, 798−807

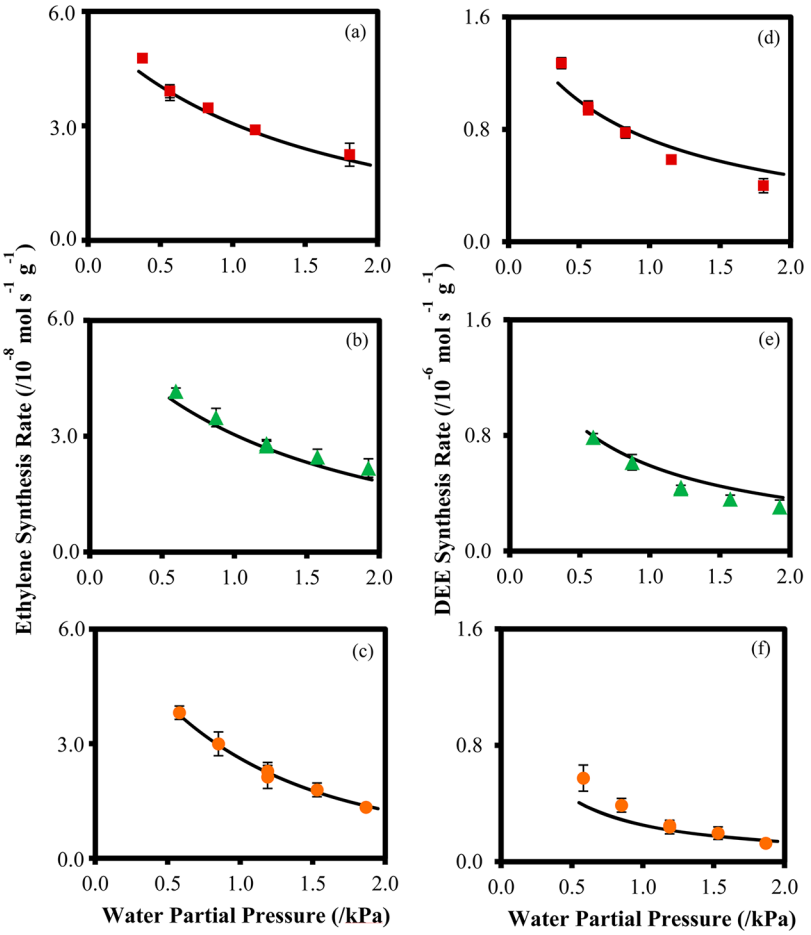

Figure 5. (a–c) Ethylene and (d–f) DEE synthesis rates for ethanol dehydration at 488 K over γ-Al_2O_3 as a function of water partial pressure with (a,d) 4.2 kPa (red squares), (b,e) 3.0 kPa (green triangles), and (c,f) 0.9 kPa (orange circles) ethanol co-feeds (total gas flow rate = 3.2 cm^3 s^{-1}). The solid lines represent fits to the experimental data with the models presented in equations (a–c) 3 and (d–f) 5.

Scheme 1. Ethoxide Desorption Limited Mechanism for Ethylene Formation from Ethanol Dehydration over γ-Al_2O_3

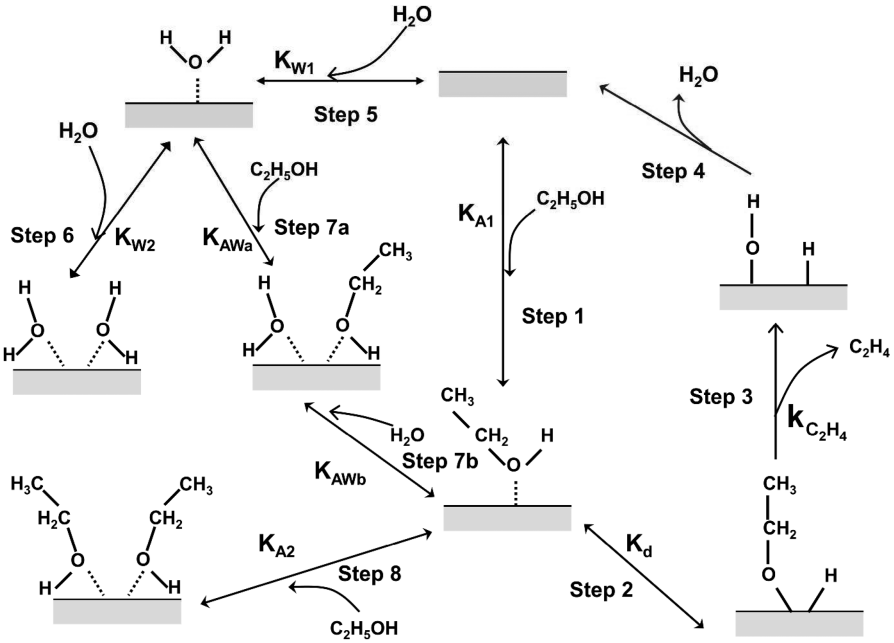

surface species. This observation, in addition to the observed differences in pyridine inhibition of the synthesis rates for the two dehydration products, leads us to postulate that the site requirements for ethylene and DEE synthesis are distinct.

dx.doi.org/10.1021/cs400051k | ACS Catal. 2013, 3, 798–807

Table 4. Estimated Values for the Kinetic Parameters of Ethylene Formation over γ-Al_2O_3 at 488 K Using the Model Presented in eq 3 and the data from Figures 4 and 5

parameter	$k_{C_2H_4}$ ($mol_{C_2H_4}$ s^{-1} g^{-1})	$K'_{AW}/(K_{A1}K_d)$ (kPa^{-1})	$K_{A1}K_{A2}/(K_{A1}K_d)$ (kPa^{-1})	$K_{W1}K_{W2}/(K_{A1}K_d)$ (kPa^{-1})
estimated value	$(6.42 \pm 0.90) \times 10^{-8}$	0.81 ± 0.27	0.035 ± 0.028	0.57 ± 0.19

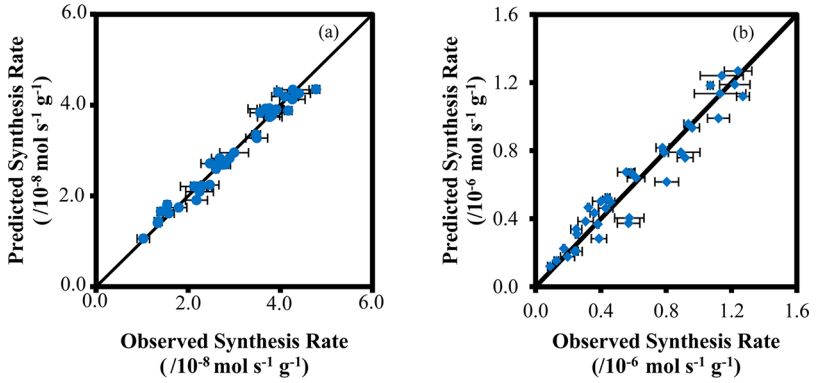

Figure 6. Parity plots for the kinetic models presented in (a) eq 3 for ethylene formation and (b) eq 5 for diethyl ether formation at 488 K. The solid line represents a perfect prediction of the observed synthesis rates.

The observed site requirements and the measured kinetic dependencies for ethylene formation can be explained with the proposed ethoxide mediated mechanism shown in Scheme 1. In this mechanism, an ethanol molecule initially adsorbs onto a Lewis acid site of γ-Al_2O_3 (Step 1, Scheme 1) and dissociates on the surface to form an ethoxide species and a hydroxyl group composed of the hydrogen atom from ethanol and a surface oxygen atom on the same Lewis acid site (Step 2, Scheme 1). The C_β-H and C_α-O bonds are subsequently cleaved as the ethoxide species desorbs from the surface to form an ethylene molecule and a hydroxyl group on the γ-Al_2O_3 surface in the rate-limiting step (Step 3, Scheme 1). Desorption of the hydroxyl group and a surface proton forms a water molecule; regenerating the catalyst surface and completing the catalytic cycle (Step 4, Scheme 1). The active site can be inhibited by the adsorption of a water molecule (Step 5, Scheme 1) along with the subsequent adsorption of an additional water or ethanol molecule to form either a water dimer (Step 6, Scheme 1) or an ethanol−water dimer (Step 7a, Scheme 1), respectively. The ethanol−water dimer could alternatively be formed from the adsorption of a water molecule onto an active site occupied by a surface bound ethanol molecule (Step 7b, Scheme 1). These two routes for the formation of the ethanol−water dimer, however, cannot be kinetically distinguished. The active site could also be inhibited by an ethanol dimer species formed from the adsorption of a second ethanol molecule after the formation of the surface bound ethanol species (Step 8, Scheme 1).

The kinetic expression for the rate of ethylene formation ($r_{C_2H_4}$) presented in eq 2 can be derived from the mechanism presented in Scheme 1 assuming quasi-equilibrium is achieved for all steps prior to the proposed rate limiting desorption of the ethylene molecule (Step 3, Scheme 1).

$$r_{C_2H_4} = k_{C_2H_4}K_{A1}K_dP_{EtOH}/\left[1 + K_{A1}K_dP_{EtOH} + K_{W1}P_{H_2O} + (K_{W1}K_{AWa} + K_{A1}K_{AWb})P_{EtOH}P_{H_2O} + K_{A1}K_{A2}P_{EtOH}^2 + K_{W1}K_{W2}P_{H_2O}^2\right] \quad (2)$$

P_{EtOH} and P_{H_2O} denote the partial pressures of ethanol and water, respectively. The kinetic parameter $k_{C_2H_4}$ represents the rate constant associated with the formation of ethylene by desorption of ethoxide species. The parameters K_{A1}, K_d, K_{A2}, K_{W1}, K_{W2} denote the equilibrium constants for the formation of adsorbed ethanol species, dissociation of the ethanol species to form a surface ethoxide species, formation of ethanol dimer complexes, the adsorption of water onto the active sites, and subsequent adsorption of additional water molecules to form water dimer complexes, respectively. K_{AWa} and K_{AWb} are the equilibrium constants for the kinetically indistinguishable routes for the formation of the ethanol−water dimers from the adsorption of an ethanol molecule to an active site occupied by a surface bound water molecule or the adsorption of a water molecule to an active site occupied by an ethanol molecule, respectively.

If surface bound ethoxide species, ethanol−water dimer species, water dimer species, and surface bound ethanol dimer species are considered to be the dominant surface species under the conditions investigated in this kinetic study, eq 2 can be simplified into eq 3.

$$r_{C_2H_4} = k_{C_2H_4}P_{EtOH}/\left[P_{EtOH} + \frac{K'_{AW}}{K_{A1}K_d}P_{EtOH}P_{H_2O} + \frac{K_{A1}K_{A2}}{K_{A1}K_d}P_{EtOH}^2 + \frac{K_{W1}K_{W2}}{K_{A1}K_d}P_{H_2O}^2\right] \quad (3)$$

The new parameter K'_{AW} represents the sum of the equilibrium constants for the two indistinguishable mechanisms for the formation of the ethanol−water dimer species ($K'_{AW} = K_{W1}K_{AWa} + K_{A1}K_{AWb}$). Equation 3 is consistent with the observation that the rate of ethylene synthesis is largely independent of ethanol pressure (between 1.9 and 7.0 kPa ethanol partial pressure and 0.4 and 2.2 kPa water partial pressure), becoming slightly of positive order only at low ethanol pressures (less than 1.9 kPa ethanol) at the highest water pressure tested (2.2 kPa), while being inhibited by water with an average order less than 1. The parameters in eq 3 were fit to the experimental data, and their values are shown in Table

dx.doi.org/10.1021/cs400051k | ACS Catal. 2013, 3, 798−807

Scheme 2. Bimolecular Mechanism for Diethyl Ether Formation from Ethanol Dehydration over γ-Al_2O_3

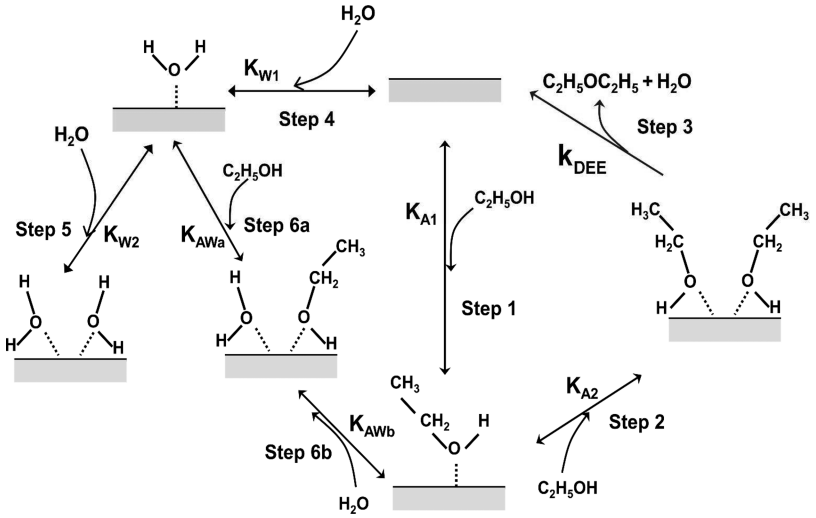

4. The parity plot of the fitted model, shown in Figure 6a, demonstrates the proposed model is capable of describing the data accurately. The normal probability plot and lag plot for the residual error in the model are presented and discussed in the Supporting Information (Figures S1a and S2a, respectively).

The value of $(K_{W1}K_{W2})/(K_{A1}K_d)$ (0.57 kPa^{-1}) relative to the value of $(K'_{AW})/(K_{A1}K_d)$ (0.81 kPa^{-1}) signifies that water dimers will become more abundant on the surface of γ-Al_2O_3 than the ethanol–water dimers when the ratio of water to ethanol pressure exceeds 1.5, which explains why a positive order dependence of ethanol on the rate of ethylene formation was observed only when the water pressure was equivalent to or exceeded the ethanol partial pressure (Figure 5a).

The lower value of $(K_{A1}K_{A2})/(K_{A1}K_d)$ (0.035 kPa^{-1}) relative to both $(K_{W1}K_{W2})/(K_{A1}K_d)$ and $(K'_{AW})/(K_{A1}K_d)$ signifies that only a small fraction of the surface is occupied with ethanol dimers except at the highest ethanol pressures and lowest water pressure tested. For this reason, the number of tested conditions in which this term is significant is much smaller than the other terms in the denominator of the rate expression which results in a relatively large confidence interval (80% of the parameter value).

The proposed desorption of the ethoxide species is consistent with the E2-like rate-limiting step for olefin formation proposed by Knözinger and Scheglila[18] based upon the observed KIE. The formation of ethoxides is supported by the observation of Greenler[30] that the infrared (IR) spectra of alumina exposed to ethanol before evacuation contained similar bands to those found in the IR spectra of $Al(OCH_2CH_3)_3$. Furthermore, Gabrienko et al.[31] observed chemical shifts indicative of the formation of alkoxide species on different Lewis acid sites in ^{13}C solid state NMR measurements of γ-Al_2O_3 exposed to ^{13}C labeled propene, *n*-butene, and isobutene (63 and 79 ppm, 69 and 74 ppm, and 67 ppm, respectively). Thus, the desorption of a surface ethoxide species (step 3) is proposed to be rate-limiting rather than the subsequent desorption of water (step 4) which could also produce the observed KIE (Section 3.3). The existence of surface ethoxides does not, however, guarantee their involvement in the synthesis of ethylene; thus, a kinetically equivalent mechanism in which the adsorbed ethanol monomer formed in step 2 directly undergoes an E2-elimination to form ethylene could also be proposed and cannot be distinguished with kinetic measurements alone.

A similar mechanism (Scheme 2) can be proposed for the formation of DEE. Initially, an ethanol molecule adsorbs onto the active site of the catalyst (Step 1, Scheme 2). The adsorption of another ethanol molecule forms an ethanol dimer complex on the surface (Step 2, Scheme 2). This dimer complex then decomposes in a rate-limiting step involving the cleavage of either a C–O or Al–O bond to form a gas phase DEE molecule and a water molecule, regenerating the catalyst surface in the process (Step 3, Scheme 2); although this process is expected to be composed of many fundamental steps, these steps are not kinetically observable. Alternatively, a water molecule can competitively adsorb onto the active site (Step 4, Scheme 2), and subsequent adsorption of an additional water molecule or an ethanol molecule forms a water dimer (Step 5, Scheme 2) or an ethanol–water dimer species (Step 6a, Scheme 2), respectively, capable of inhibiting the rate of DEE formation. As was the case with ethylene formation, the ethanol–water dimer could alternatively be formed from the adsorption of a water molecule onto a site occupied by a surface bound ethanol molecule (Step 6b, Scheme 2).

Equation 4 shows the kinetic expression for the rate of DEE formation (r_{DEE}) derived from the proposed mechanism.

$$r_{DEE} = k_{DEE}K_{A1}K_{A2}P_{EtOH}^2/\Big[1 + K_{A1}P_{EtOH} + K_{W1}P_{H_2O} + (K_{W1}K_{AWa} + K_{A1}K_{AWb})P_{EtOH}P_{H_2O} + K_{A1}K_{A2}P_{EtOH}^2 + K_{W1}K_{W2}P_{H_2O}^2\Big] \quad (4)$$

The rate constant for DEE formation is denoted by k_{DEE}. Equation 4 can be simplified into eq 5 assuming that ethanol–water and ethanol dimer species are more abundant than the other surface species depicted in Scheme 2.

$$r_{DEE} = \frac{k_{DEE}P_{EtOH}^2}{P_{EtOH}^2 + \frac{K'_{AW}}{K_{A1}K_{A2}}P_{EtOH}P_{H_2O}} \quad (5)$$

The rate expression presented in eq 5 can describe the observed less than 1 order reaction order in ethanol pressure on the rate of DEE formation and the observation that the order decreased with increasing ethanol pressure and decreasing

dx.doi.org/10.1021/cs400051k | ACS Catal. 2013, 3, 798–807

water pressure until becoming independent of ethanol pressure. The parameters in eq 5 were estimated with a Bayesian fit to the experimental data collected at 488 K and are shown in Table 5. The model accurately describes the data between 0.9 and 3.0 kPa in ethanol partial pressure and between 1.2 and 2.2 kPa water partial pressures as well as describing the zero order regime at ethanol pressures >4.5 kPa and at a water pressure of 0.4 kPa (Figures 4b and 5b). The parity plot for the model and the collected data is presented in Figure 6b. The normal probability plot and lag plot associated with the residual error in the model are presented and discussed in the Supporting Information (Figures S1b and S2b, respectively).

Table 5. Estimated Values for the Kinetic Parameters of DEE Formation over γ-Al_2O_3 at 488 K Using the Model Presented in eq 5 and the Data from Figures 4 and 5

parameter	k_{DEE} (mol_{DEE} s^{-1} g^{-1})	$(K'_{AW})/(K_{A1}K_{A2})$
estimated value	$(1.60 \pm 0.18) \times 10^{-6}$	5.05 ± 1.24

The value of the combined parameter $(K'_{AW})/(K_{A1}K_{A2})$ (5.05) signifies that, under the experimental conditions, ethanol−water dimers are the most abundant surface species unless the ethanol pressure is 4 or more times greater than the water pressure, explaining why the rate of DEE formation was found to be independent of ethanol partial pressure only when the ethanol partial pressure was an order of magnitude larger than the water partial pressure.

Pyridine titration studies elucidated both the acidic and the nonequivalent nature of the active sites for the formation of ethylene and DEE; whether the active sites consist of a single adsorption site or two adjacent adsorption sites, however, could not be determined based upon kinetic experiments or pyridine titration studies alone. The ethanol dimers, water dimers, and ethanol−water dimers could represent either two molecules adsorbed onto the same adsorption site, as shown to form on acidic zeolites,[32−34] or adsorbed onto two adjacent adsorption sites both of which are necessary for the formation of ethylene and DEE and comprise the active site for dehydration. These two possibilities, however, are kinetically equivalent and, thus, cannot be distinguished using the information presented in this work. The existence of two adjacent adsorption sites has been previously suggested by De Mourgues et al.[23] to explain the observed independence in isopropanol pressure and simultaneous inhibition by water for the rate of propene formation from isopropanol dehydration over γ-Al_2O_3. De Mourges et al.[23] proposed that one site exclusively adsorbs ethanol, while the other is exclusively inhibited by water. De Mourges's model, however, does not allow for the inhibition of olefin formation by water dimers and, thus, is unable to fully explain the observed −1.6 order inhibition of the rate of ethylene synthesis by water at the lowest ethanol pressure (0.9 kPa) and highest measured water pressures (1.5 and 1.9 kPa).

The measured inhibitory effects of water and the kinetic effects of ethanol for ethylene and DEE synthesis demonstrate the kinetic importance of water, ethanol−water, and ethanol molecular pairs, either in the form of adsorbed dimers or in the form of molecules adsorbed on adjacent active sites, in the dehydration of ethanol over γ-Al_2O_3. The observed inhibition by ethanol−water dimers for both ethylene and DEE formation on Lewis-acidic γ-Al_2O_3 was not observed for the same chemistry performed over Brønsted acidic zeolite catalysts,[32] highlighting the important fundamental mechanistic differences between these catalytic systems. Our findings demonstrate the kinetic importance of molecular dimers for the dehydration of ethanol over γ-Al_2O_3 and provide important considerations for future catalytic research with this common catalytic system.

4. CONCLUSIONS

Kinetic measurements of ethanol dehydration over γ-Al_2O_3 at 488 K on both samples exposed to water before reaction and untreated samples established water is capable of irreversibly deactivating some of the active sites involved in the formation of both ethylene and DEE. Steady state kinetic measurements on samples treated with water demonstrated water is capable of reversibly inhibiting the rate of both ethylene and DEE synthesis on the remaining active sites. Pyridine and ethanol co-feed kinetic experiments indicated pyridine reversibly inhibits the rate of ethylene and DEE formation to different extents, demonstrating the active sites for ethylene and DEE formation are acidic and nonequivalent. In-situ pyridine titration studies estimated 2.7×10^{-5} mol g^{-1} of pyridine are required to adsorb onto the surface of water-treated γ-Al_2O_3 to completely deactivate the synthesis of DEE; this value provides an upper estimate of active site density for the formation of DEE (0.10 sites nm^{-2}). A primary kinetic isotope effect was observed for the rate of ethylene formation when C_2D_5OD was used as the reactant but not when C_2H_5OD was employed, indicating the rate-limiting step for ethylene formation from ethanol dehydration over γ-Al_2O_3 involves either the cleavage of a C−H bond (likely the acidic C_β-H bond) of ethanol or the subsequent desorption of water from the surface of γ-Al_2O_3. No significant kinetic isotope effect was observed for the rate of DEE formation for either of the deuterated reactants, elucidating the formation of DEE from ethanol dehydration over γ-Al_2O_3 is limited by either C_α-O or Al−O bond cleavage. Steady state kinetic measurements of the formation of ethylene and DEE at various ethanol and water partial pressures at 488 K demonstrated the following: (1) the rate of ethylene formation was independent of ethanol pressure for most of the ethanol and water pressures tested while being inhibited by water, (2) the rate of DEE formation was found to be a positive, less than first order dependence in ethanol pressure except at very high ethanol pressure and low water pressures where the rate of DEE formation became independent of ethanol pressure, and (3) the order of the inhibition by water decreased with increasing ethanol pressure for both ethylene and DEE formation. The proposed mechanisms and associated rate equations, in which, at the reaction conditions, the formation of ethylene and DEE is inhibited mostly by bimolecular surface species, are consistent with the experimental observations.

■ ASSOCIATED CONTENT

Supporting Information

Analysis of the residual error in the kinetic models for ethanol dehydration. This material is available free of charge via the Internet at http://pubs.acs.org.

■ AUTHOR INFORMATION

Corresponding Author

*E-mail: abhan@umn.edu. Phone: 612-626-3981. Fax: 612-626-7246.

Author Contributions

§Equal contribution to this work was given by these authors.

Notes

The authors declare no competing financial interest.

■ ACKNOWLEDGMENTS

We thank The Dow Chemical Company for their financial support. H.C. was supported as part of the Catalysis Center for Energy Innovation, an Energy Frontier Research Center funded by the U.S. Department of Energy, Office of Science, Office of Basic Energy Sciences under Award no. DE-SC0001004.

■ REFERENCES

(1) Chorkendorff, I.; Niemantsverdriet, J. W. *Concepts of Modern Catalysis and Kinetics*; Wiley-VCH: Weinheim, Germany, 2007.
(2) Kogel, J. E.; Trivedi, N. C.; Barker, J. M. *Industrial Minerals & Rocks: Commodities,Markets, and Uses*; Society for Mining Metallurgy: Littleton, CO, 2006.
(3) Lippens, B. C.; De Boer, J. H. *Acta Crystallogr.* **1964**, *17*, 1312−1321.
(4) Slade, R. C. T.; Southern, J. C.; Thompson, I. M. *J. Mater. Chem.* **1991**, *1*, 563−568.
(5) Cesteros, Y.; Salagre, P.; Medina, F.; Sueiras, J. E. *Chem. Mater.* **1999**, *6*, 123−129.
(6) Winfield, M. E. In *Catalysis*; Emmett, P. H., Ed.; Reinhold: New York, 1960; Vol. *VII*.
(7) Knözinger, H. *Angew. Chem., Int. Ed. Engl.* **1968**, *7*, 791−805.
(8) Coster, D.; Blumenfeld, A. L.; Fripiat, J. J. *J. Phys. Chem.* **1994**, *98*, 6201−6211.
(9) Morterra, C.; Magnacca, G. *Catal. Today* **1996**, *27*, 497−532.
(10) Liu, X.; Truitt, R. E. *J. Am. Chem. Soc.* **1997**, *119*, 9856−9860.
(11) Parry, E. P. *J. Catal.* **1963**, *2*, 371−379.
(12) Soled, S. L.; McVicker, G. B.; Murrell, L. L.; Sherman, L. G.; Dispenziere, N. C., Jr.; Hsu, S. L.; Waldman, D. *J. Catal.* **1988**, *295*, 286−295.
(13) Baertsch, C. D.; Komala, K. T.; Chua, Y. H.; Iglesia, E. *J. Catal.* **2002**, *205*, 44−57.
(14) Ripmeester, J. A. *J. Am. Chem. Soc.* **1983**, *105*, 2925−2927.
(15) Kwak, J.; Hu, J.; Kim, D.; Szanyi, J.; Peden, C. *J. Catal.* **2007**, *251*, 189−194.
(16) Kwak, J. H.; Mei, D.; Peden, C. H. F.; Rousseau, R.; Szanyi, J. *Catal. Lett.* **2011**, *141*, 649−655.
(17) Pines, H.; Haag, W. O. *J. Am. Chem. Soc.* **1961**, *82*, 1526−1532.
(18) Knözinger, H.; Scheglila, A. *J. Catal.* **1970**, *17*, 252−263.
(19) Knözinger, H.; Bühl, H.; Kochloefl, K. *J. Catal.* **1972**, *24*, 57−68.
(20) Knözinger, H.; Bühl, H.; Ress, E. *J. Catal.* **1968**, *12*, 121−128.
(21) Kalló, D.; Knözinger, H. *Chem.-Ing. Techn.* **1967**, *39*, 676−680.
(22) Shi, B.; Davis, B. H. *J. Catal.* **1995**, *157*, 359−367.
(23) De Mourgues, L.; Peyron, F.; Trambouze, Y.; Prettre, M. *J. Catal.* **1967**, *7*, 117−125.
(24) Roy, S.; Mpourmpakis, G.; Hong, D. Y.; Vlachos, D. G.; Bhan, A.; Gorte, R. J. *ACS Catal.* **2012**, *2*, 1846−1853.
(25) Digne, M.; Sautet, P.; Raybaud, P.; Euzen, P.; Toulhoat, H. *J. Catal.* **2002**, *211*, 1−5.
(26) Digne, M.; Sautet, P.; Raybaud, P.; Euzen, P.; Toulhoat, H. *J. Catal.* **2004**, *226*, 54−68.
(27) Wischert, R.; Laurent, P.; Copéret, C.; Delbecq, F.; Sautet, P. *J. Am. Chem. Soc.* **2012**, *134*, 14430−14449.
(28) Zotov, R. a.; Molchanov, V. V.; Volodin, A. M.; Bedilo, A. F. *J. Catal.* **2011**, *278*, 71−77.
(29) Knözinger, H.; Scheglila, A.; Watson, A. M. *J. Phys. Chem.* **1968**, *72*, 2770−2774.
(30) Greenler, R. G. *J. Chem. Phys.* **1962**, *37*, 2094−2100.
(31) Gabrienko, A. A.; Arzumanov, S. S.; Toktarev, A. V.; Stepanov, A. G. *J. Phys. Chem. C* **2012**, *116*, 21430−21438.
(32) Chiang, H.; Bhan, A. *J. Catal.* **2010**, *271*, 251−261.
(33) Zecchina, A.; Bordiga, S.; Spoto, G.; Scarano, D.; Spano, G.; Geobaldo, F. *J. Chem. Soc., Faraday Trans.* **1996**, *92*, 4863−4875.
(34) Lee, C. C.; Gorte, R. J.; Farneth, W. E. *J. Phys. Chem. B* **1997**, *101*, 3811−3817.